PHYSICAL REVIEW B **84**, 121411(R) (2011)

Observation of anomalous peaks in the photoelectron spectra of highly oriented pyrolytic graphite: Folding of the band due to the surface charge density wave transition

S. Tanaka,[1,*] M. Matsunami,[2,3] and S. Kimura[2,3]

[1]*The Institute of the Industrial and Scientific Research, Osaka University, 567-0047 Mihogaoka, Ibaraki, Osaka, Japan*

[2]*UVSOR Facility, Institute for Molecular Science, Okazaki 444-8585, Japan*

[3]*School of Physical Sciences, The Graduate University for Advanced Studies, Okazaki 444-8585, Japan*

(Received 13 July 2011; published 26 September 2011)

The angle-resolved photoelectron spectroscopy with low-photon energy (7–16 eV) is used for the investigation of highly oriented pyrolytic graphite at a low temperature. We observed for the first time peaks in the low binding energy region (from the Fermi level to 0.7 eV) of the surface normal photoelectron spectra at 11K, which disappear above ∼30K. Based on the dispersion both along the parallel and normal to the surface, the peaks are ascribed to the emission from the K(H)-point that is backfolded into the Γ(A)-point as a result of the two-dimensional superperiodicity. The surface charge density wave transition is proposed for the driving mechanism of the superperiodicity based on the temperature dependence of the photoelectron intensity.

DOI: 10.1103/PhysRevB.84.121411 PACS number(s): 79.60.−i, 71.45.Lr

Graphite has been regarded as a "textbook" system for solid state physics for many years because of its unique characteristics. A single layer of graphite is of a pure two-dimensional (2D) nature and commonly called a graphene sheet, which consists of hexagonal lattices bonded with sp^2-hybridized orbital. The interlayer interaction is weaker than the intralayer interaction; thus, the 3D graphite can be considered a quasi-2D system. The highly symmetric points of the 2D Brillouin zone (BZ) are at the center (Γ), the corner (K), and the edge center (M) points of the hexagonal zone (see Fig. 2(c) later in the chapter), and the corresponding points at the edge face of the 3D-BZ are the A-, H-, and L-points, respectively. Theoretical[1,2] and angle-resolved photoelectron spectroscopy (ARPES)[3–8] studies revealed the electronic structures of the graphite, where the π-bands cross the Fermi energy (E_F) at the corner (K-H) of the BZ, and there is a band gap of several electron volts in the center of the BZ (Γ-A). Although each graphene sheet is azimuthally disordered in highly oriented pyrolytic graphite (HOPG), Zhou *et al*. demonstrated that the ARPES can be performed to obtain the band dispersions in the high-symmetry directions [Γ–M (A–L) and Γ–K (A–H)] of the BZ thanks to the complete angular averaging.[7]

In this study, we investigate the electronic structures of HOPG at low temperatures using the ARPES with the tunable photon energy of 7–16 eV, which is lower than that reported in most previous research.[3–8] Generally, when the final state energy of the photoexcitation is smaller, the photoelectron spectrum is influenced more effectively by the electronic properties of the solid.[9] In other words, it is difficult to apply the nearly free electron approximation to the final state of the photoexcitation. Thus, much information about not only the initial state but also the final state can be derived from the low-photon energy photoelectron spectroscopy. Moreover, by using a strong resonance effect in the photoelectron emission as a result of the optical transition, it may be possible to observe efficiently a specific electron state by tuning the photon energy.

The ARPES experiments were carried out at the BL7U SAMRAI of the UVSOR-II, the synchrotron radiation facility at the Institute for Molecular Science.[10] The typical instrumental resolution was 12 meV at $h\nu = 11.5$ eV, and the incident angle of the p-polarized light was 50° from the surface normal. The angular resolution of the photoelectron detection was 0.18°. The photon intensity was calibrated with the photodiode. The MgF_2 filter is used when the photon energy was lower than 10.9 eV to reduce the higher-order light. The HOPG sample was freshly cleaved with an adhesive tape in the ultrahigh vacuum system of $\sim 7\times10^{-9}$ Pa, where the ARPES measurements are made. The reliability of the whole experiments was checked by comparing our ARPES results of HOPG using higher photon energies (typically $h\nu =$ 41 eV) with the previous results.[3–8] The sample temperature was controlled by the flow rate of the liquid He for the cryostat. When the temperature dependence of the spectra was measured, the sample was cooled at an average rate of 0.1 K/min. The change in temperature during each ARPES measurement was <0.3 K, as the flow rate of the liquid He remained nearly constant during the measurement.

Figure 1(a) shows a series of normal-emission photoelectron spectra of HOPG at 11 K using the photon energies from 7.3 to 16 eV (0.3-eV step). The acceptance angle for the photoelectron was 0.18°. Electron energies are referred with respect to E_F, which was determined with the Au film. A distinct peak just below the Fermi level is visible when the photon energy is near 11.5 eV with a relatively high intensity. Moreover, a smaller peak at the binding energy (E_B) ≈ 0.7 eV is observed when the photon energy is near 12.1 eV, and its binding energy changes as a function of the photon energy. These are displayed more clearly in Fig. 1(b), where the spectra in the region of 0–1.2 eV are shown for several photon energies. In Fig. 1(c), photoelectron intensities at $E_B = 0.02$, 0.3, and 0.7 eV are plotted as a function of the photon energy (solid dots). The so-called constant initial state (CIS) spectroscopy shows the probability for the optical transition from an occupied state of the given E_B into a final state as a function of the excitation energy, enabling an energy mapping of the unoccupied states.[11] The experimental results can be well described by the sum of two Lorentzian curves shown as solid lines. The peak position and width for the component of the lower photon energy are, respectively, 11.5 and 0.86 eV at $E_B = 0.02$ eV, 11.70 and 1.09 eV at $E_B = 0.3$ eV, and 12.19 and 0.92 eV at

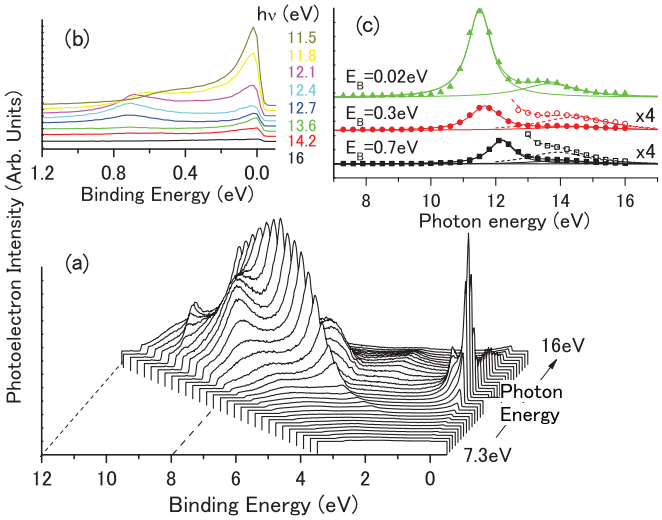

FIG. 1. (Color online) (a) A series of the photoelectron spectra with various photon energies at 11 K. Electron emission along the surface normal is measured. (b) Photoelectron spectra taken with several photon energies. (c) The intensities as a function of the photon energy for the photoelectrons whose binding energies are 0.02 eV (solid triangles), 0.3 eV (solid squares), and 0.7 eV (solid circles). The lines show the calculated curves with two Lorentzian peaks. The four-times magnified curves (open squares and circles with dotted lines) are also shown for $E_B = 0.3$ and 0.7 eV.

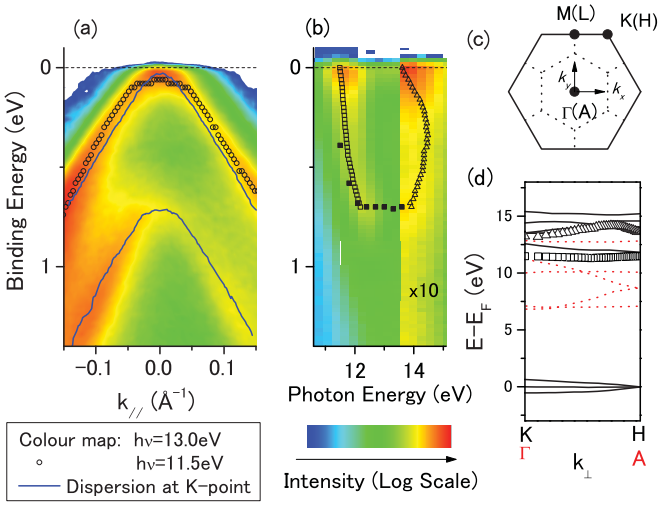

FIG. 2. (Color online) (a) The ARPES intensity map in the logarithmic scale at $h\nu = 13$ eV taken at 11 K. Open circles show the dispersions of the peaks obtained from the ARPES spectra at $h\nu = 11.5$ eV, and the (blue) line shows the dispersion of the π-band near the K-point of the single-crystal graphite according to the previous ARPES result (Ref. 6). (b) The surface-normal photoelectron intensity map in logarithmic scale as a function of the binding energy and the photon energy. The intensities at $h\nu > 13.3$ eV are multiplied by 10. Open squares and triangles represent peak positions (see text). (c) The 2D ($k_z = 0$) BZ for the graphite (solid lines). The dotted lines illustrate the zone folding associated with a $p(\sqrt{3} \times \sqrt{3})R30^\circ$ superperiodicity. (d) The dispersion along k_z of the unoccupied states derived from the open squares and triangles in (b) and the calculated dispersion curves for the K-H (solid black lines) and the Γ-A (dotted red lines) directions (Ref. 2).

$E_B = 0.7$ eV. Those for the higher photon energy are 13.65 and 2.08 eV at $E_B = 0.02$ eV, 14.43 and 2.82 eV at $E_B = 0.3$ eV, and 13.93 and 2.22 eV at $E_B = 0.7$ eV. As the components of the higher photon energy are so small in intensity at $E_B = 0.3$ and 0.7 eV, the magnified curves are also shown in the figure. These photoelectron and CIS spectra indicate the detection of the photoelectron emission near E_F with a high efficiency is due to the specific optical transitions from the occupied electronic states into the unoccupied states, the details of which are discussed later.

In the normal emission, only electron states along the Γ-A line of the BZ can be observed. Therefore, the peaks at $E_B \approx 0$ and 0.7 eV in the ARPES spectra [Fig. 1(a) and 1(b)] are paradoxical since, as noted earlier, the band crosses E_F near the K-point, and no corresponding bands near E_F have been reported at the center of the BZ.[1–8] Thus, in this study, we concentrate on these anomalous peaks, and only tentative interpretations are made for the other peaks as follows. The largest peaks, whose binding energy linearly shifts with the photon energy (e.g., $E_B = 6.6$ eV at $h\nu = 14.2$ eV), are due to the secondary electron peaks with a constant kinetic energy.[3] The peaks at ∼8 and ∼4.5 eV (shifted slightly as a function of the photon energy) are attributed to the π- and σ-bands, respectively, at the Γ-point. The small peak at ∼2.7 eV is same as the e_1 peak in Ref. 7. The origin of the peaks at 9.7 eV is discussed later.

To obtain the information about the two anomalous peaks shown in Fig. 1(b), we measured the band dispersion by using ARPES at 11 K. In Fig. 2(a), the dispersions of these peaks as a function of $k_{//}$ (inverse vector parallel to the surface) are displayed. The color map shows photoelectron intensity taken at $h\nu = 13$ eV, and the open circles indicate the peak positions in the ARPES spectra at 11.5 eV. The figure shows that the dispersions of the two peaks closely resemble those of the π-bands around the K-point in the k_y direction (defined in Fig. 2(c), i.e., the K-M-K′ direction) in the single-crystalline graphite,[6] which are displayed as solid lines in Fig. 2(a). Since each graphene sheet is azimuthally disordered in HOPG, the dispersion along $k_{//}$ is averaged in azimuth angle, as stated earlier. A slight discrepancy between the present results for HOPG and that in the single crystal may be due to the anisotropy in the dispersion of these bands,[8] as well as the difference in the photon energy. The agreement in the dispersions suggests that the anomalous peaks observed at the Γ(A)-point have the same origin as the π-bands at the K(H)-point. This interpretation is supported by the detailed measurements of the photon-energy dependence for the surface normal photoelectron emission shown in Fig. 2(b), where the color map shows the photoelectron intensity as functions of electron binding energy and the photon energy (the intensities at $h\nu > 13.3$ eV are multiplied by 10). For evaluating the binding and photon energies corresponding to a specific photoexcitation, we used the CIS spectra, examples of which were shown in Fig. 1(c) . The open squares and triangles in Fig. 2(b) are derived from the peak positions of the Lorentzian curves fitted for the CIS spectra at given binding energies. The positions of the symbols sometimes disagree with intense positions in the color map of Fig. 2(b) at $h\nu > 13.3$ eV because of an overlapping with the tail

of the stronger peak at $h\nu \approx 12$ eV [see Fig. 1(c)]. Peak positions in the photoelectron spectra [see Fig. 1(b)] at given photon energies are also shown as solid squares in Fig. 2(b). The 2D energy positions in Fig. 2(b) are determined by the momentum-conservation law in the optical transition from the two initial (occupied) bands into two final (unoccupied) bands [as shown in Fig. 1(b) and 1(c)], both of which may be dispersed along the surface normal k_z. The position in E_B of the strong peak just below E_F is nearly constant, which is evident in Figs. 1(a) and 1(b). This flat branch of $E_B \approx 0$ intersects at $h\nu = 11.5$ eV ($h\nu = 13.65$ eV) with the branch shown as open squares (open triangles) that disperses with a band width of ~0.7 eV. This indicates that one of the relevant occupied bands has nearly a flat dispersion and the other has a dispersion from 0 to ~0.7 eV along k_z. This is the case for the π-bands at the corner of the BZ along the K-H line (k_z direction) of graphite, shown as solid lines[2] in Fig. 2(d); a single band at the H-point splits into three bands (one occupied, one unoccupied, and one weakly dispersing across E_F) along the K-H line. The agreement suggests again that the anomalous peaks originated from the π-band at the K(H)-point of the graphite. Then, we can determine the dispersions of the two final (unoccupied) bands along k_z by assuming the dispersions of the occupied bands are similar to the π-band along the K-H line that is known.[2,6] The unoccupied bands located at ~11.5 eV (open squares) and ~14 eV (open triangles) from E_F in Fig. 2(d) are deduced from the branches at $h\nu \approx 12$ eV (open squares) and ≈14 eV (open triangles), respectively, in Fig. 2(b). Although the obtained dispersions of the unoccupied bands seem to approximate the calculated bands[2] along K-H lines (solid lines) rather than Γ-A lines (dotted lines), we cannot make unambiguous assignments for the unoccupied bands since the calculation for the dispersions of the unoccupied bands is not well established compared with that for the occupied ones.[12]

The similarity between the dispersions of the anomalous peaks and the π-bands at K(H)-points in both $k_{//}$ and k_z directions clearly excludes the assignment to the defect,[7] edge,[5] or surface states, and these peaks are unambiguously ascribed to electron emission from the π-band at the K(H)-point of the graphite. The electron at the K-point might be scattered to the Γ-point via electron–phonon scattering, which couples with photoexcitation. We can, however, reject this interpretation, because (1) it is inconsistent with these peaks being observed only at low temperatures, as shown later, despite the higher phonon population at higher temperatures, and (2) electron–phonon scattering has to be accompanied by energy loss (gain) due to phonon emission (absorption), as demonstrated by Liu *et al.*[13] which is inconsistent with the sharp edge exactly located at E_F observed in the present case. Therefore, it is considered that the K-point of HOPG at 11 K is backfolded into the Γ-point as a result of the formation of the superperiodicity of $p(\sqrt{3} \times \sqrt{3})R30^\circ$ or larger, which is schematically shown as dotted lines in Fig. 2(c). The detection of the photoelectron emission from the K-point at the surface normal can be provided by the diffraction (scattering) by the reciprocal lattice vector of the 2D superlattice. The formation of the superperiodicity is also supported by the observation of the peak at 9.7 eV in the surface normal photoelectron spectra [see Fig. 1(a)], which is assigned to the σ-band at the K-point. The observation of electron emission from the backfolded K-point was previously reported in the graphite intercalated compound (GIC), where the $p(\sqrt{3} \times \sqrt{3})R30^\circ$ superperiodicity is formed due to the intercalated atom.[14–16] The electron structure of the GIC is not significantly different from that of the graphite except for a folding of the 2D-BZ and an energy shift due to the carrier doping from the intercalated atoms, where a backfolded π-band from the K-point crosses the Fermi level near the Γ-point.[14–16] In the present case, however, there are no intercalated atoms, and the superperiodicity cannot be ascribed to the intercalation. We examined three HOPG samples, and these two peaks were always observed at 11K. Moreover, they were observed on the sample ~30 hours after the cleaving, as well as on the freshly cleaved sample. Thus, the superperiodicity cannot be ascribed to the extrinsic impurities such as adsorbed gas molecules on the surface.

We measured the sample temperature dependence of the photoelectron spectra to reveal the condition for the superperiodicity formation. Figure 3 shows a series of the surface normal photoelectron spectra of HOPG at $h\nu = 11.5$ eV while the sample was cooled. When the sample was >30 K, almost no photoelectron emission is observed in the spectral region of 0–0.8 eV. By decreasing the temperature, the intensity of the photoelectron emission increases in this energy region without a significant change in the spectral shape. We found that this change in intensity is reversible; these peaks are extinguished when the sample is warmed and then reappear when it is cooled. In the inset of Fig. 3, the photoelectron intensity at $E_B = 0.016$ eV (solid circles) is plotted as a function of the reduced temperature (the temperature divided by the critical temperature $T_C = 29$ K). The temperature dependence is similar to that of the x-ray reflection intensity corresponding to the superlattice formation as a result of the charge density wave (CDW) transition, examples of which are shown for $NbSe_3$ ($T_C = 59$ K, upward open triangles),[17] $(TaSe_4)_2I$ ($T_C = 260$ K,

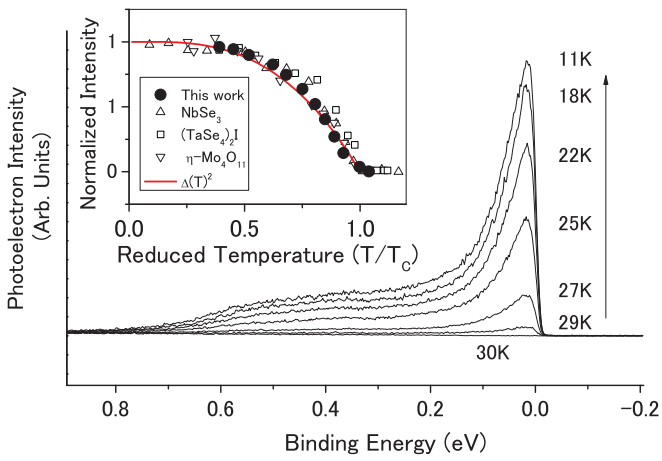

FIG. 3. (Color online) Surface normal photoelectron spectra of HOPG at various temperatures of the sample ($h\nu = 11.5$ eV). In the inset, solid circles are photoelectron intensities of HOPG at $B_E = 0.016$ eV as a function of the reduced temperature (divided by T_C of 29 K), and other dots are the superlattice reflection intensities of x ray as a result of the CDW transition in various materials (Refs. 17–19). The solid line is a square of the BCS-type order parameter (Ref. 20).

open squares),[18] and η-Mo_4O_{11} ($T_C = 107$ K, downward open triangles).[19] Since the detection of the photoelectron emission from the K-point at the surface normal is a result of the diffraction (scattering) of the electron by the reciprocal lattice vector of the superlattice, this is indeed a proper comparison. The solid curve in the inset of Fig. 3 gives the square of the order parameter Δ predicted by the Bardeen, Cooper, and Schrieffer (BCS) law, which is phenomenologically approximated as $\Delta(T) = \Delta_0 \tanh(1.74\sqrt{\frac{T_C}{T} - 1})$, where Δ_0 is the value at $T = 0$, and reproduces all experimental results despite the variety in T_C.[20] Consequently, it is strongly suggested that the formation of the superlattice in HOPG is caused by the CDW transition. We may argue that the CDW formation should accompany the opening of the gap at k_F, which is not observable in the present case (Fig. 3). According to the study with the ARPES for 2H-$TaSe_2$,[21] however, the CDW gap does not open at E_F but at a different point of the BZ. Thus, the absence of the gap at E_F does not necessarily exclude the possibility of the CDW transition.

The CDW transition in the graphite was proposed to explain a sharp increase in magnetoresistance at 3 K in a strong magnetic field.[22] To the best of our knowledge, this study is the first experimental report for the CDW transition in graphite without a magnetic field.[23] What we have to take into account is that no macroscopic physical properties such as the specific heat,[24] thermal conductivity,[25] or electrical resistivity[25] have any singularities ~30 K. The CDW transition might contradict previous knowledge on graphite, since these properties should be affected by the CDW formation[20] if the transition occurred in the bulk of HOPG. Therefore, the superperiodicity may be formed at the surface or the layers near the surface. The probing depth under the present experimental condition is estimated to be 40 Å (about 12 layers of graphene), because electron kinetic energy is ~6 eV.[9] Although this is larger than the ordinal photoelectron spectroscopy due to the lower photon energy, the probing volume is still limited near the surface from a macroscopic view. The $p(\sqrt{3} \times \sqrt{3})R30^\circ$ superlattice has been observed on the graphite surface with the scanning tunneling microscopy at various temperatures.[26] The $p(\sqrt{3} \times \sqrt{3})R30^\circ$ superlattice on the surface was observed near the defect and step edge, relatively large coverage of which is observed on HOPG surfaces cleaved by adhesive tape.[27] At this stage, however, the detail of the superperiodicity formation at HOPG < 29 K is not clear; thus, further research, e.g., the temperature dependence of electron diffraction, is required.

In summary, we found anomalous peaks just below E_F at the surface normal photoelectron spectra of HOPG at the temperature <30 K whose intensity is resonantly enhanced at 11.5 eV with a narrow width for the first time. Based on the dispersion measurements, these are assigned to the π-band at the K(H)-point of the 2D-BZ, which is backfolded into the Γ(A)-point as a result of the formation of the superperiodicity of $p(\sqrt{3} \times \sqrt{3})R30^\circ$or larger. From the temperature dependence of the photoelectron intensity, the CDW transition is proposed as the driving force of the superperiodicity formation. This observation demonstrates the advantage of the photoelectron spectroscopy with the tunable photons of the low energy.

The present work was partly carried out at the UVSOR facility under the Joint Studies Program of the Institute for Molecular Science.

*stanaka@sanken.osaka-u.ac.jp

[1] J. M. McClure, Phys. Rev. **108**, 612 (1957).
[2] R. C. Tatar and S. Rabii, Phys. Rev. B **25**, 4126 (1982).
[3] D. Marchand, C. Frétigny, M. Laguës, F. Batallan, C. Simon, I. Rosenman, and R. Pinchaux, Phys. Rev. B **30**, 4788 (1984).
[4] V. N. Strocov, A. Charrier, J.-M. Themlin, M. Rohlfing, R. Claessen, N. Barrett, J. Avila, J. Sanchez, and M.-C. Asensio, Phys. Rev. B **64**, 075105 (2001).
[5] K. Sugawara, T. Sato, S. Souma, T. Takahashi, and H. Suematsu, Phys. Rev. B **73**, 045124 (2006).
[6] A. Grüneis, C. Attaccalite, T. Pichler, V. Zabolotnyy, H. Shiozawa, S. L. Molodtsov, D. Inosov, A. Koitzsch, M. Knupfer, J. Schiessling, R. Follath, R. Weber, P. Rudolf, L. Wirtz, and A. Rubio, Phys. Rev. Lett. **100**, 037601 (2008).
[7] S. Y. Zhou, G.-H. Gweon, C. D. Spataru, J. Graf, D.-H. Lee, S. G. Louie, and A. Lanzara, Phys. Rev. B **71**, 161403 (2005).
[8] S. Y. Zhou, G.-H. Gweon, J. Graf, A. V. Fedorov, C. D. Spataru, R. D. Diehl, Y. Kopelevich, D.-H. Lee, S. G. Louie, and A. Lanzara, Nat. Phys. **2**, 595 (2006).
[9] S. Hüfner, *Photoelectron Spectroscopy* (Springer-Verlag, Berlin, 2010).
[10] S. Kimura, T. Ito, M. Sakai, E. Nakamura, N. Kondo, T. Horigome, K. Hayashi, M. Hosaka, M. Katoh, T. Goto, T. Ejima, and K. Soda, Rev. Sci. Instrum. **81**, 053104 (2010).
[11] A. Bianconi, S. B. M. Hagström, and R. Z. Bachrach, Phys. Rev. B **16**, 5543 (1977).
[12] F. Maeda, T. Takahashi, H. Ohsawa, S. Suzuki, and H. Suematsu, Phys. Rev. B **37**, 4482 (1988).
[13] Y. Liu, L. Zhang, M. K. Brinkley, G. Bian, T. Miller, and T.-C. Chiang, Phys. Rev. Lett. **105**, 136804 (2010).
[14] W. Eberhardt, I. T. McGovern, E. W. Plummer, and J. E. Fischer, Phys. Rev. Lett. **44**, 200 (1980).
[15] S. Y. Leung and G. Dresselhaus, Phys. Rev. B **24**, 3490 (1981).
[16] S. L. Molodtsov, F. Schiller, S. Danzenbächer, M. Richter, J. Avila, C. Laubschat, and M. C. Asensio, Phys. Rev. B **67**, 115105 (2003).
[17] R. M. Fleming, D. E. Moncton, and D. B. McWhan, Phys. Rev. B **18**, 5560 (1978).
[18] H. Fujishita, M. Sato, and S. Hoshino, Solid State Commun. **49**, 313 (1984).
[19] H. Guyot, C. Schlenkert, J. P. Pougetf, R. Ayroles, and C. Roucau, J. Phys. C: Solid State Phys. **18**, 4427 (1985).

[20]G. Grüner, Rev. Mod. Phys. **60**, 1129 (1988).
[21]R. Liu, C. G. Olson, W. C. Tonjes, and R. F. Frindt, Phys. Rev. Lett. **80**, 5762 (1998).
[22]D. Yoshioka and H. Fukuyama, J. Phys. Soc. Jpn. **50**, 725 (1981).
[23]A commensurate CDW has been predicted to form for a graphene bilayer: H. P. Dahal, T. O. Wehling, K. S. Bedell, J.-X. Zhu, and A. V. Balatsky, Phys. B Condens. Matter **405**, 2241 (2010).
[24]W. DeSorbo and W. W. Tyler, J. Chem. Phys. **21**, 1660 (1953).
[25]W. W. Tyler and A. C. Wilson Jr., Phys. Rev. **89**, 870 (1953).
[26]W-T. Pong and C. Durkan, J. Phys. D Appl. Phys. **38**, R329 (2005), and references therein.
[27]H. Chang and A. J. Bard, Langmuir **7**, 1143 (1991).